Degenerate Two-Photon Absorption in All-Trans Retinal: Nonlinear Spectrum and Theoretical Calculations

M. G. Vivas,[†] D. L. Silva,[†] L. Misoguti,[†] R. Zaleśny,[‡] W. Bartkowiak,[‡] and C. R. Mendonca*[,†]

Instituto de Física de São Carlos, Universidade de São Paulo, Caixa Postal 369, 13560-970 São Carlos, SP, and Theoretical Chemistry Group, Institute of Physical and Theoretical Chemistry, Wrocław University of Technology, Wybrzeøe Wyspiańskiego 27, 50-370 Wrocław, Poland

Received: October 19, 2009; Revised Manuscript Received: January 19, 2010

In this work we investigate the degenerate two-photon absorption spectrum of all-trans retinal in ethanol employing the Z-scan technique with femtosecond pulses. The two-photon absorption (2PA) spectrum presents a monotonous increase as the excitation wavelength approaches the one-photon absorption band and a peak at 790 nm. We attribute the 2PA band to the mixing of states $^1B_u^+$-like and $|S_1\rangle$, which are strongly allowed by one- and two-photon, respectively. We modeled the 2PA spectrum by using the sum-over-states approach and obtained spectroscopic parameters of the electronic transitions to $|S_1\rangle$, $|S_2\rangle$ ("$^1B_u^+$"), $|S_3\rangle$, and $|S_4\rangle$ singlet-excited states. The results were compared with theoretical predictions of one- and two-photon transition calculations using the response functions formalism within the density functional theory framework with the aid of the CAM-B3LYP functional.

1. Introduction

All-trans retinal (ATR) is a polyene chromophore of foremost relevance in the light transduction process in nervous impulses. Its charge redistribution is associated with a significant change in dipole moment.[1−3] In the last few decades, ATR was exhaustingly studied for applications in optoelectronic devices due to its ultrafast isomerization in bacteriorhodopsin.[4−7] However, there is still a small number of studies on the third-order nonlinear optical properties of ATR, in particular, those that allow the direct measurement of the nonlinear absorption coefficient, such as the Z-scan technique,[8] for instance.

Pioneering studies of nanosecond up-conversion fluorescence and theoretical analysis carried out by Birge[1,3] revealed that the three low-lying excited singlet states of ATR are of $n\pi^*$, $^1A_g^-$-like ($\pi\pi^*$), and $^1B_u^+$-like ($\pi\pi^*$) characters, respectively. Excited-state ordering is important to define the photochemical properties of the ATR chromophore in solution. Nevertheless, so far there is no consensus on the order of the electronic states involved in one- and two-photon transitions of ATR, mainly because of the distinct molecular conformation and polarity exhibited by ATR in different solvents.[9,10] Two-photon induced fluorescence results[1] revealed a red shift between the two-photon and the linear absorption band, indicating the presence of a two-photon allowed state near "$^1B_u^+$". Ultrafast transient absorption[9] and femtosecond fluorescence up-conversion spectroscopy[6] have contributed to the understanding of the electronic states involved in the photophysics of ATR. More recently, Yamaguchi and Tahara[11] have used femtosecond pump−probe technique to measure the 2PA spectrum of ATR in hexane. A red shift was also observed in the 2PA peak with respect to the one-photon absorption, which was attributed to an allowed 2PA state. Hence, the study of ATR using different experimental approaches seems to be of foremost importance to comprehend its photophysical processes.

* Corresponding author. E-mail: crmendon@ifsc.usp.br.
[†] Universidade de São Paulo.
[‡] Wrocław University of Technology.

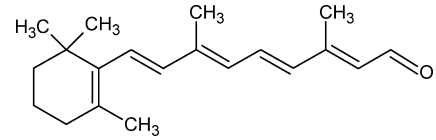

Figure 1. Molecular structure of the all-trans retinal.

To help the understanding of the electronic states of ATR, we study its degenerate two-photon absorption spectrum in ethanol, using the open aperture Z-scan technique with femtosecond pulse excitation. In an effort to further comprehend the two-photon absorption spectrum of ATR, we carried out theoretical calculations using the quadratic response function formalism within the density functional theory (DFT) framework, which allowed the determination of the lowest two-photon allowed states of the chromophore.

2. Experimental Section

We prepared ATR/ethanol solutions with concentrations of 1.65×10^{-3} and 3.5×10^{-2} mol L^{-1}, for linear and nonlinear optical measurements, respectively. ATR was purchased from Sigma-Aldrich. The ATR molecular structure is presented in Figure 1. The samples were placed in 2 mm thick quartz cuvettes for the optical measurements. The linear absorption spectrum was recorded using a Cary 17 UV−vis−NIR spectrophotometer. The two-photon absorption spectrum was obtained using the Z-scan technique.[8]

In the Z-scan technique, the two-photon absorption cross-section is determined by translating the sample through the focal plane of a focused Gaussian beam, while changes in the far field intensity are monitored. For a 2PA process, the light field creates an intensity dependent absorption, $\alpha = \alpha_0 + \beta I$, where I is the laser beam intensity, α_0 is the linear absorption coefficient, and β is the two-photon absorption coefficient. Far from one-photon resonances, the power transmitted through the sample due to a two-photon absorption process, for each wavelength, is integrated over time (assuming a pulse with a

10.1021/jp910010g
Published on Web 02/15/2010

Gaussian temporal profile) to give the normalized energy transmittance,[8]

$$T(z) = \frac{1}{\sqrt{\pi} q_o(z,0)} \int_{-\infty}^{\infty} \ln[1 + q_o(z,0)e^{-\tau^2}]\, d\tau \qquad (1)$$

with

$$q_o = \beta I_o L(1 + (z^2/z_o^2))^{-1} \qquad (2)$$

where L is the sample thickness, z_0 is the Rayleigh length, z is the sample position, and I_0 is the laser intensity. The nonlinear coefficient β is obtained by fitting the Z-scan data with eq 1. The two-photon absorption cross-section, δ, is determined from $\delta = h\nu\beta/N$, where $h\nu$ is the excitation photon energy, and N is the number of molecules per cm^3. Usually, the two-photon absorption cross-section is expressed in units of Göppert-Mayer (GM), where 1 GM $= 1 \times 10^{-50}$ cm^4 $\times$ s $\times$ mol^{-1} $\times$ photon^{-1}.

Nonlinear optical measurements were carried out by employing 120 fs laser pulses from an optical parametric amplifier pumped by 150 fs pulses at 775 nm delivered by a Ti:sapphire chirped pulse amplified system, operating at 1 kHz repetition rate. The Z-scan measurements were carried out with intensities ranging from 25 to 90 GW/cm^2. The Z-scan setup is the same as that described in a previous publication.[12] All the measurement and sample preparations were performed in a dark room at room temperature. No photodegradation was observed for the ATR/ethanol solution after nonlinear optical measurements for the intensities used.

3. Results

The one-photon absorption spectrum of ATR in ethanol is presented in Figure 2a (gray line). Such a linear absorption spectrum can be decomposed (Gaussian decomposition) in three bands (dashed line in Figure 2a), corresponding to three $\pi\pi^*$ transitions, with absorption maxima at 250, 300, and 385 nm. The circles in Figure 2a represent the two-photon absorption spectrum of ATR determined by performing open-aperture Z-scan measurements similar to the ones presented in Figure 3a at three distinct wavelengths. The decrease observed in the normalized transmittance as a function of the z position in Figure 3a indicates a 2PA process, since excitation took place in nonresonant conditions. In Figure 3, the solid lines represent the theoretical fitting obtained with eq 1, from which we were able to determine the 2PA cross-section (δ) as a function of the excitation wavelength. In Figure 3b, we show the linear dependence observed for the transmittance change (ΔT) as a function of the excitation laser irradiance at 790 nm. Such behavior is typical of a two-photon absorption process[12] and it was observed for all excitation wavelengths investigated (from 530 to 900 nm).

The 2PA spectrum (Figure 2a, circles) presents a monotonous increase as the excitation wavelength approaches the one-photon absorption band and a peak in 790 nm. Figure 2b shows a comparison between the one- and two-photon absorption spectra (the two-photon absorption data were plotted as a function of half-excitation wavelength). One can clearly observe that the two-photon absorption band is red-shifted by about 10 nm in comparison to the one-photon absorption band, indicating that the state accessed by the absorption of two-photons does not correspond, necessarily, to the state accessed by one photon. Moreover, the line width of the two-photon spectrum is smaller,

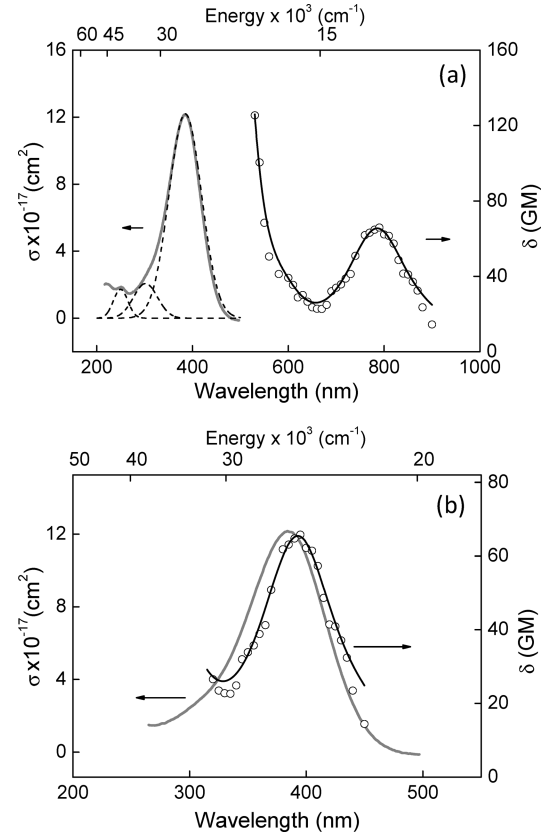

Figure 2. (a) (Dashed lines) Gaussian decomposition of the 1PA spectrum. (Solid line) theoretical fitting obtained with the SOS approach to 2PA spectrum. (b) Comparison of the one-photon (gray line) and degenerate two-photon absorption spectra (circles-solid line) of all-trans retinal in ethanol. The 2PA spectrum data were plotted as a function of the half-excitation wavelength.

in energy, than the one-photon spectrum, corroborating the previous hypothesis.

To gain an insight into ATR electronic states and help to interpret its two-photon absorption spectrum, we performed quantum-chemical calculations. Due to the size of the investigated system, all computations were carried out using the density functional theory (DFT).[13] The Gaussian 03 program[14] was used to determine the equilibrium geometry of the molecule with the aid of the Becke's three-parameter exchange functional in combination with the LYP correlation functional (B3LYP)[15] and the standard 6-31G(d) basis set.[16] Figure 4 shows the equilibrium geometry of ATR. It is observed that the ATR is not planar, with the polyene chain out of the plane of β-ionone ring. This conformation is attributed to intramolecular steric repulsion between the hydrogen of the ring and the polyene chain.[17]

Subsequently, to characterize the lowest allowed 1PA and 2PA states of ATR, the response functions formalism,[18] within the DFT framework, was used as implemented in the DALTON program.[19] In this approach, the oscillator strengths and two-photon transition probabilities are calculated analytically as single residues of the linear and quadratic response functions of the molecular electronic density, respectively. All electronic transition computations were carried out by employing the recently developed Coulomb-attenuated hybrid functional (CAM-B3LYP)[20] and the 6-31+G(d) basis set.[16] In particular, the CAM-B3LYP functional used here applies the long-range correction recommend by Tawada et al.[21] to better describe long-range charge distribution modifications, an important point for accurately determine the electronic transitions of the investigated

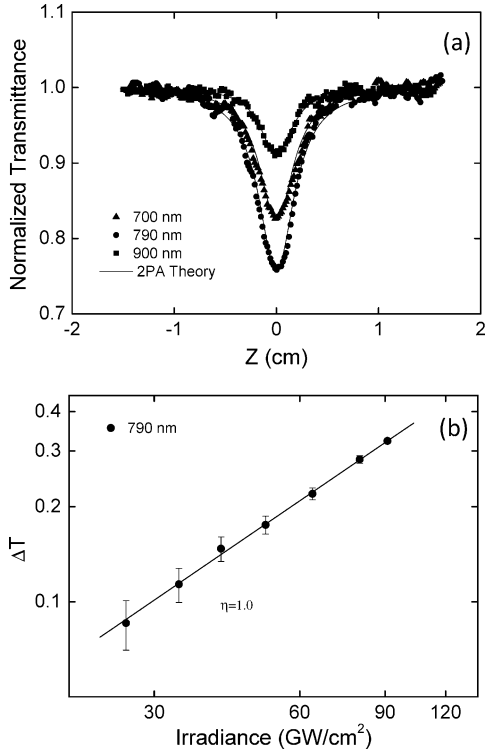

Figure 3. (a) Open-aperture Z-scan curves for ATR in ethanol, performed with an intensity of 85 GW/cm^2, at three different excitation wavelengths. The solid lines represent the theoretical fittings obtained with eq 1. (b) Plots of normalized transmittance variation (ΔT) vs irradiance at 790 nm (log−log scale). The solid line is the linear fit with a slope of $\eta = 1.0$, which indicates the 2PA process.

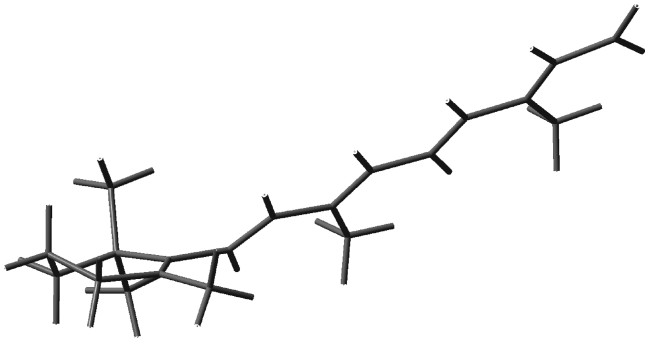

Figure 4. Ground-state equilibrium geometry of all-trans retinal optimized at the DFT level of theory (B3LYP/6-31G(d)).

molecule (charge transfer transitions). All computations were carried out in vacuo, without taking into account any solvent effect. Table 1 presents the results obtained from 1PA and 2PA calculations for ATR using the CAM-B3LYP functional and the 6-31+G(d) basis set. As shown by electronic transition calculations (Table 1), ATR presents three distinct electronic states (defined as S_2, S_3 and S_4), which are allowed in one- and two-photon absorption processes. The excitation energies corresponding to the S_2, S_3, and S_4 states, calculated in vacuum, were 368, 270, and 250 nm, respectively (Table 1). The S_2 and S_3 states deviate about 20 nm from the ones obtained by Gaussian decomposition (Figure 2a). It is well-known that $\pi\pi^*$ transitions of polyene chromophores present a high red shift in a polar solvent such as ethanol.[10] When theoretical values are compared with results for the ATR in nonpolar solvent (hexane: main band in 3.3 eV (375 nm) and two additional weaker transitions at approximately 4.4 (282 nm) and 5 eV (248 nm)),[1,22] better agreement is obtained.

TABLE 1: Results of 1PA and 2PA Calculations for All-Trans Retinal Using the Response Functions Formalism and the Approach CAM-B3LYP/6-31+G(d)[a]

	1PA		2PA		
state	energy (eV)	oscillator strength	energy (eV)	transition probability (au)	2PA cross-section (GM)
S_2 ($\pi\pi^*$)	3.37	1.2244	3.37 (368 nm)	20000	22
S_3 ($\pi\pi^*$)	4.59	0.2033	4.59 (270 nm)	32800	51
S_4 ($\pi\pi^*$)	4.97	0.0855	4.97 (250 nm)	155000	391
S ($n\pi^*$)	3.54	0.0001	3.54 (350 nm)	0.475	

[a] The 2PA cross-sections were estimated by considering the line widths obtained through the decomposition (Gaussian decomposition) of the linear spectrum.

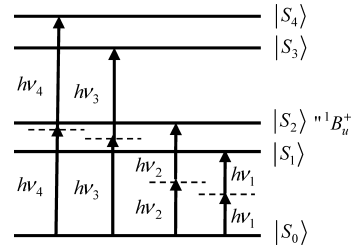

Figure 5. Energy level diagram of low single-excited states of all-trans retinal used to fit the two-photon absorption spectrum utilized in the SOS approach.

To further understand the 2PA spectrum and its connection with the molecular properties, we employed the sum-over-states (SOS) approach.[23] As a first attempt to model the 2PA spectrum of ATR, we considered a four-level-energy diagram based on the energy states obtained by quantum chemistry calculations and linear absorption data (S_2, S_3, and S_4). Nevertheless, considering only these three states, we were unable to obtain a satisfactory fitting of the 2PA spectrum. However, as indicated by the results presented in Figure 2b, there might be another two-photon allowed state near S_2 ("$^1B_u^+$" state) which contributes to the 2PA process.[1,6,10] Following this hypothesis, we proposed a five-level-energy diagram (Figure 5), which includes a two-photon allowed S_1 state (supposed to be less energetic than S_2), to describe the 2PA spectrum under the SOS approach. As reported by Birge et al.,[1] the origin of the S_1 state is strongly related with the molecular conformation of ATR, which is affected by the solvent environment and temperature. This is the probable reason why it was not observed in the quantum chemical calculations presented here. The n $\rightarrow \pi^*$ transition (Table 1) was neglected in the SOS model because this transition is extremely weak for both one- and two-photons absorption processes.[1] In this case, the SOS expression used to fit the 2PA spectrum is given by

$$\delta(\nu) = \frac{4}{5\pi}\frac{(2\pi)^4}{(hc)^2}\left\{\frac{|\mu_{01}|^2\Delta\mu_{01}{}^2\Gamma_{01}}{(\nu_{01}-2\nu)^2+\Gamma_{01}{}^2} + \frac{|\mu_{02}|^2\Delta\mu_{02}{}^2\Gamma_{02}}{(\nu_{02}-2\nu)^2+\Gamma_{02}{}^2} + \left[\frac{\nu^2}{(\nu_{02}-\nu)^2+\Gamma_{02}{}^2}\times\left(\frac{|\mu_{02}|^2|\mu_{23}|^2\Gamma_{03}}{(\nu_{03}-2\nu)^2+\Gamma_{03}{}^2} + \frac{|\mu_{02}|^2|\mu_{24}|^2\Gamma_{04}}{(\nu_{04}-2\nu)^2+\Gamma_{04}{}^2}\right)\right]\right\} \quad (3)$$

where h is Planck's constant, c is the speed of light and ν is the excitation laser frequency. ν_{nm}, Γ_{nm}, and μ_{nm} represent, respectively, the transition frequency, damping constant, and transition

TABLE 2: Spectroscopic Parameters Used/Obtained in the SOS Approach[a]

spectroscopic parameters	SOS model
ν_{01} (cm^{-1})	25290 (395 ± 5 nm)
ν_{02} (cm^{-1})	25940 (385 ± 2 nm)
ν_{03} (cm^{-1})	33350 (300 ± 2 nm)
ν_{04} (cm^{-1})	39960 (250 ± 2 nm)
Γ_{01} (cm^{-1})	4485 (70 ± 5 nm)
Γ_{02} (cm^{-1})	5530 (82 ± 2 nm)
Γ_{03} (cm^{-1})	6440 (58 ± 2 nm)
Γ_{04} (cm^{-1})	5760 (36 ± 2 nm)
μ_{01} (Debye)	3.5 ± 1 (f_{01} = 0.15 ± 0.08)
μ_{02} (Debye)	9.0 ± 0.5 (f_{02} = 1.0 ± 0.1)
μ_{23} (Debye)	2.6 ± 0.5
μ_{24} (Debye)	6.5 ± 0.5
$\Delta\mu_{01}$ (Debye)	12 ± 2
$\Delta\mu_{02}$ (Debye)	4 ± 1

[a] f_{01} and f_{02} are the oscillator strengths of transitions to the states S_1 and S_2, respectively.

dipole moments corresponding to the n → m transition. In this expression $\Delta\mu_{01} = \mu_{11} - \mu_{00}$ and $\Delta\mu_{02} = \mu_{22} - \mu_{00}$ are the difference between the permanent dipole moment of excited ($|S_1\rangle$ and $|S_2\rangle$) and the ground states, respectively. In eq 3, the terms inside curly brackets stand for the normalized 2PA line shapes and can be separated into two dipolar contributions, corresponding to two-photon transitions to the $|S_1\rangle$ and $|S_2\rangle$ states, and two two-photon terms related to the higher $|S_3\rangle$ and $|S_4\rangle$ excited states, which are affected by a resonance enhancement of the nonlinearity. For the resonance enhancement factor (term multiplying the parentheses in the square brackets) we assumed that only one intermediate state, $|S_2\rangle$ (1PA allowed), contributes to the virtual intermediate state.

The solid line in Figure 2a represents the fitting obtained using eq 3 with ν_{02}, ν_{03} and ν_{04} taken from the linear absorption spectrum ($\pi\pi^*$ bands located at 385, 300, and 250 nm, respectively), and μ_{02} estimated from the 1PA peak amplitude.[24] The values of Γ_{02} = 5530 cm^{-1} (82 nm), Γ_{03} = 6440 cm^{-1} (58 nm), and Γ_{04} = 5760 cm^{-1} (36 nm) were obtained from the linear absorption spectrum (Figure 2a) through the Gaussian decomposition.[25] From the fitting we were able to determine ν_{01} and Γ_{01}, the transition dipole moments μ_{01}, μ_{23}, and μ_{24}, and the dipole moment changes $\Delta\mu_{01}$ and $\Delta\mu_{02}$. Table 2 summarizes the spectroscopic parameters used/obtained in the SOS model.

According to the five-level-energy diagram proposed here, the 2PA band at 790 nm is described by transitions to the states $|S_2\rangle$ ("$^1B_u^+$") and $|S_1\rangle$, with the main contribution coming from $|S_1\rangle$ (70%). Such contributions can be estimated by the amplitude of each term in eq 3. The two-photon transitions $S_0 \rightarrow S_2$, $S_0 \rightarrow S_3$, and $S_0 \rightarrow S_4$ are only allowed for noncentrosymmetric molecules such as ATR, where the two-photon electric-dipole selection rules are relaxed.[26] In this case, 2PA takes place by a mechanism in which a change in the dipole moment occurs upon excitation from the ground state to an excited state. As the laser frequency approaches the one-photon transition, the two-photon absorption tensor and the two-photon transition to the higher energy state $|S_4\rangle$ increase their contribution, resulting in the enhancement of the nonlinearity.[23]

As mentioned previously, Birge et al.,[1] using two-photon induced fluorescence with nanosecond pulses, observed a red shift on the 2PA spectrum with respect to the linear absorption. Such a result, obtained at low temperature (77 K) and on ethyl−ether−isopentane−alcohol was attributed to a two-photon allowed state near "$^1B_u^+$". Yamaguchi and Tahara[11] studied the 2PA spectrum of ATR (in hexane) using femtosecond time-resolved pump−probe. They observed a red shift of approximately 7 nm in the 2PA band in comparison to the one-photon band, which was also attributed to an allowed 2PA state. In that work, the authors estimated the 2PA cross-section on the order of 200 GM. Such a value is about 3 times higher than the ones reported here, probably due to a resonant enhancement of the nonlinearity achieved in ref 11 when the probe wavelength beam approaches the one-photon absorption of ATR. Therefore, the experimental results we obtained with the degenerate Z-scan technique as well as the interpretation of the 2PA spectrum, assuming a two-photon allowed state below "$^1B_u^+$", are in agreement with these pioneer studies.[1,10,11]

The relatively small 2PA cross-section values determined for ATR, experimentally (Figure 2) and theoretically (Table 1), are probably related to the low planarity of the ground-state equilibrium geometry[27,28] and the absence of strong electron acceptor or -donnor on the chromophore.[29]

4. Conclusion

In this paper, we reported the degenerate two-photon absorption cross-section spectrum of ATR, a potential material for development of biophotonic devices, in ethanol by using the open-aperture Z-scan technique with femtosecond pulses. We modeled the nonlinear spectrum by using the sum-over-states approach and obtained spectroscopy parameters of the electronic transitions to $|S_1\rangle$, $|S_2\rangle$ ("$^1B_u^+$"), $|S_3\rangle$, and $|S_4\rangle$ singlet-excited states, comparing the results with theoretical predictions for one- and two-photon transition calculations using the response functions formalism within the DFT framework. We associated the 2PA peak (790 nm) with a mixing of the states $|S_2\rangle$ ("$^1B_u^+$") and $|S_1\rangle$, strongly allowed by one- and two-photon absorption, respectively. Such interpretation of the 2PA spectrum of ATR is in agreement with previous studies performed with different experimental techniques and excitation pulses.[1,10,11] This study helps to understand the nature of the nonlinear absorption process in ATR.

Acknowledgment. Financial support from FAPESP (Fundação de Amparo à Pesquisa do estado de São Paulo), CNPq (Conselho Nacional de Desenvolvimento Científico e Tecnológico), Coordenação de Aperfeiçoamento de Pessoal de Nível Superior (CAPES), the Air Force Office of Scientific Research (FA9550-07-1-0374), and the European Commission through the Human Potential Programme (Marie-Curie RTN BIMORE, Grant No. MRTN-CT-2006-035859) are gratefully acknowledged. We also gratefully acknowledge the allotment of the CPU time in Wroclaw Center of Networking and Supercomputing (WCSS). R.Z. is the recipient of the fellowship co-financed by European Union within European Social Fund.

References and Notes

(1) Birge, R. R.; Bennett, J. A.; Hubbard, L. M.; Fang, H. L.; Pierce, B. M.; Kliger, D. S.; Leroi, G. E. *J. Am. Chem. Soc.* **1982**, *104*, 2519.
(2) Birge, R. R.; Bocian, D. F.; Hubbard, L. M. *J. Am. Chem. Soc.* **1981**, *104*, 1196.
(3) Birge, R. R.; Pierce, B. M. *J. Chem. Phys.* **1979**, *70*, 165.
(4) Gai, F.; Hasson, K. C.; McDonald, J. C.; Anfinrud, P. A. *Science* **1998**, *279*, 1886.
(5) Hampp, N. *Chem. Rev.* **2000**, *100*, 1755.
(6) Takeuchi, S.; Tahara, T. *J. Phys. Chem. A* **1997**, *101*, 3052.
(7) Zgrablic', G.; Voýtchovsky, K.; Kindermann, M.; Haacke, S.; Chergui, M. *Biophys. J.* **2005**, *88*, 2779.
(8) Sheik-Bahae, M.; Said, A. A.; Wei, T.-H.; Hagan, D. J.; Stryland, E. W. V. *IEEE J. Quantum Electron.* **1990**, *26*, 760.
(9) Larson, E. J.; Friesen, L. A.; Johnson, C. K. *Chem. Phys. Lett.* **1997**, *265*, 161.

(10) Larson, E. J.; Pyszczynski, S. J.; Johnson, C. K. *J. Phys. Chem. A* **2001**, *105*, 8136.

(11) Yamaguchi, S.; Tahara, T. *J. Chem. Phys. Lett.* **2003**, *376*, 237.

(12) Boni, L. D.; Andrade, A. A.; Correa, D. S.; Balogh, D. T.; Zilio, S. C.; Misoguti, L.; Mendonca, C. R. *J. Phys. Chem. B* **2004**, *108*, 5221.

(13) Hohenberg, P.; Kohn, W. *Phys. Rev. B* **1964**, *136*, B864.

(14) Frisch, M. J.; Schlegel, H. B.; Scuseria, G. E.; Robb, M. A.; Cheeseman, J. R.; Montgomery, J. A., Jr.; Vreven, T.; Kudin, K. N.; Burant, J. C.; Millam, J. M.; Iyengar, S. S.; Tomasi, J.; Barone, V.; Mennucci, B.; Cossi, M.; Scalmani, G.; Rega, N.; Petersson, G. A.; Nakatsuji, H.; Hada, M.; Ehara, M.; Toyota, K.; Fukuda, R.; Hasegawa, J.; Ishida, M.; Nakajima, T.; Honda, Y.; Kitao, O.; Nakai, H.; Klene, M.; Li, X.; Knox, J. E.; Hratchian, H. P.; Cross, J. B.; Adamo, C.; Jaramillo, J.; Gomperts, R.; Stratmann, R. E.; Yazyev, O.; Austin, A. J.; Cammi, R.; Pomelli, C.; Ochterski, J. W.; Ayala, P. Y.; Morokuma, K.; Voth, G. A.; Salvador, P.; Dannenberg, J. J.; Zakrzewski, V. G.; Dapprich, S.; Daniels, A. D.; Strain, M. C.; Farkas, O.; Malick, D. K.; Rabuck, A. D.; Raghavachari, K.; Foresman, J. B.; Ortiz, J. V.; Cui, Q.; Baboul, A. G.; Clifford, S.; Cioslowski, J.; Stefanov, B. B.; Liu, G.; Liashenko, A.; Piskorz, P.; Komaromi, I.; Martin, R. L.; Fox, D. J.; Keith, T.; Al-Laham, M. A.; Peng, C. Y.; Nanayakkara, A.; Challacombe, M.; Gill, P. M. W.; Johnson, B.; Chen, W.; Wong, M. W.; Gonzalez, A.; Pople, P. A. *Gaussian03*; Gaussian Inc.: Pittsburgh, PA, 2003.

(15) Becke, A. D. *J. Chem. Phys.* **1993**, *98*, 5648.

(16) Frisch, M. J.; Pople, J. A.; Binkley, J. S. *J. Chem. Phys.* **1984**, *80*, 3265.

(17) Honig, B.; Hudson, B.; Sykes, B. D.; Karplus, M. *Proc. Natl. Acad. Sci. U.S.A.* **1971**, *68*, 1289.

(18) Salek, P.; Vahtras, O.; Guo, J. D.; Luo, Y.; Helgaker, T.; Agren, H. *Chem. Phys. Lett.* **2003**, *374*, 446.

(19) DALTON a molecular electronic structure program, Release 2.0 (2005), see http://www.kjemi.uio.no/software/dalton/dalton.html.

(20) Yanai, T.; Tew, D. P.; Handy, N. C. *Chem. Phys. Lett.* **2004**, *393*, 51.

(21) Tawada, Y.; Tsuneda, T.; Yanagisawa, S.; Yanai, T.; Hirao, K. *J. Chem. Phys.* **2004**, *120*, 8425.

(22) Merchán, M.; González-Luque, R. *J. Chem. Phys.* **1996**, *106*, 1112.

(23) Kamada, K.; Ohta, K.; Iwase, Y.; Kondo, K. *Chem. Phys. Lett.* **2003**, *372*, 386.

(24) Paul, N.; Day, K. A. N.; Pachter, R. *J. Phys. Chem. B* **2005**, *109*, 1803.

(25) Zucchelli, G.; Dainese, P.; Jennings, R. C.; Breton, J.; Garlaschi, F. M.; Bassi, R. *Biochemistry* **1994**, *33*, 8982.

(26) Bonin, K. D.; McIlrath, T. J. *J. Opt. Soc. Am. B* **1984**, *1*, 52.

(27) Reinhardt, B. A.; Brott, L. L.; Clarson, S. J.; Dillard, A. G.; Bhatt, J. C.; Kannan, R.; Yuan, L. X.; He, G. S.; Prasad, P. N. *Chem. Mater.* **1998**, *10*, 1863.

(28) De Boni, L.; Piovesan, E.; Misoguti, L.; Zilio, S. C.; Mendonca, C. R. *J. Phys. Chem. A* **2007**, *111*, 6222.

(29) Albota, M.; Beljonne, D.; Bredas, J. L.; Ehrlich, J. E.; Fu, J. Y.; Heikal, A. A.; Hess, S. E.; Kogej, T.; Levin, M. D.; Marder, S. R.; McCord-Maughon, D.; Perry, J. W.; Rockel, H.; Rumi, M.; Subramaniam, C.; Webb, W. W.; Wu, X. L.; Xu, C. *Science* **1998**, *281*, 1653.

JP910010G